

Supporting Information (SI)

Interplay of deformability and adhesion on localization of elastic micro-particles in blood flow

Huilin Ye¹, Zhiqiang Shen¹ and Ying Li^{1,2,†}

¹Department of Mechanical Engineering, University of Connecticut, 191 Auditorium Road, Unit 3139, Storrs, Connecticut 06269, United States

²Institute of Materials Science, University of Connecticut, 97 North Eagleville Road, Unit 3136, Storrs, Connecticut 06269, United States

1. Motion of spherical MP in bi-shear flow

We place a single spherical MP in the center of a channel with dimension $L_x \times L_y \times L_z = 10D_p \times 10D_p \times 10D_p$. $D_p = 2\mu\text{m}$ is the diameter of the MP. We apply periodic boundary conditions in the x and z directions. y -direction is bounded by two flat plates. The bi-shear flow is driven by the moving of flat plates with opposite velocities U_0 . Under the bi-shear flow, the MP will deform and make tank-treading motion. We use two parameters to quantify the deformation and motion of MP. One is the Taylor parameter D_{xy} , which is defined as: $D_{xy} = (a - b)/(a + b)$. a and b are semi-major and semi-minor axes of the MP, respectively. The other one is the inclination angle of the MP between major axis of MP and flow direction (x -direction) as shown in figure 1(a). We conduct two cases for MP with different deformability $Ca = 0.0125$ and $Ca = 0.125$. We compare the results of Taylor parameter and inclination angle with those in Lac et al. (2004). We find that our simulation results are in good agreement with the previous computational study by Lac et al. (2004). It further confirms that the modeling of MP is accurate enough using current computational model.

† Email address for correspondence: yingli@enr.uconn.edu

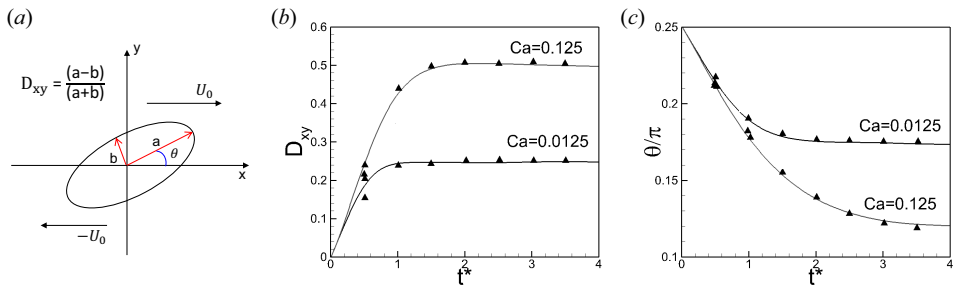


Figure 1. Motion of a spherical MP in bi-shear flow. (a) Computational model. a and b are semi-major and semi-minor axes of the MP, respectively. U_0 is the plate velocity. θ is the inclination angle of MP between major axis and flow direction (x-direction). The Taylor parameter D_{xy} is defined as $D_{xy} = (a - b)/(a + b)$. (b) The influence of Capillary number Ca on Taylor parameter D_{xy} . (c) The influence of Capillary number Ca on inclination angle θ . Solid triangles denote experimental results in Lac et al. (2004) and lines are the present simulation results.

2. Morse Potential Calibration

Interactions between RBCs are modeled using the Morse potential (Liu & Liu 2006; Fedosov et al. 2011; Tan et al. 2012):

$$U_{morse} = D_0[e^{-2\beta(r-r_0)} - 2e^{-\beta(r-r_0)}], r < r_c, \quad (2.1)$$

where D_0 represents the energy well depth and β controls the width of potential well, r is the distance between two particles and r_0 is the equilibrium distance, r_c is the cutoff distance. In our computational model, $\beta = 2 \mu\text{m}^{-1}$, $r_0 = 0.5 \mu\text{m}$, and $r_c = 1.5 \mu\text{m}$. The energy well depth D_0 is calibrated by separation test. As studied by Fedosov et al. (2011), we apply pulling forces between two RBCs. One of them is fixed on the substrate, and we pull the upper one in the normal direction. The force is 7 pN and we distribute this force uniformly on 200 vertexes on the membrane. We change the energy well depth D_0 . Through a series of tests, we obtain the critical D_0 , under which we can separate these two RBCs. Because the Morse potential is a pair-wise potential. It is applied between vertexes (c.f. figure 2(a)). The discretization of the membrane should affect the critical D_0 . We change the discretization of the membrane and obtain the critical D_0 as shown in figure 2(c). It is found that the critical D_0 decreases with increase of vertex number. Assuming there are N_a vertex in upper RBC which will interact with the lower RBC, and every vertex in N_a can interact with N_b vertexes in lower RBC. Hence, the total interaction strength between upper and lower RBCs is $D_0 \times N_a \times N_b$. N_a and N_b monotonically increase with the increase of vertexes of the RBC membrane. Thus, the critical D_0 may linearly decrease with square root of the membrane vertexes increasing. Then it can ensure the total interaction strength between two RBCs keeps the same. This can also be reflected by figure 2(c).

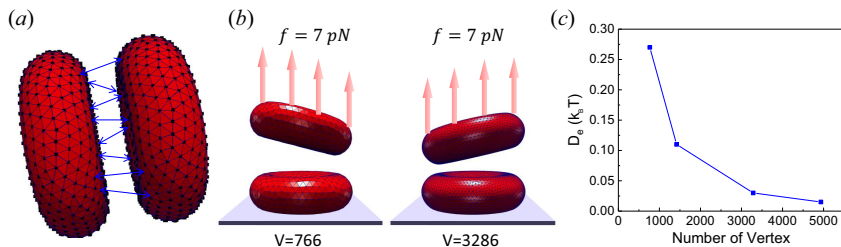


Figure 2. Morse potential calibration. (a) Interaction mode applied by Morse potential. (b) Separation test between two RBCs under 7 pN pulling force with different vertexes of the membrane. (c) Critical energy well depth D_0 against discretization of membrane (number of vertex).

3. Thickness of the CFL

To validate the numerical method and computational model, the calculation of the cell-free layer (CFL) thickness is conducted for hematocrit $Ht = 10\%$ and 20% . We place 48 and 96 RBCs for $Ht = 10\%$ and 20% respectively in the channel with dimension $L_x \times L_y \times L_z = 27 \mu\text{m} \times 54 \mu\text{m} \times 36 \mu\text{m}$. x -direction and y -direction are applied with periodical boundary conditions. z -direction is bounded by two fixed flat plates. Poiseuille flow in the channel is driven by the pressure difference between inlet and outlet in y -direction. As the simulation progresses, the CFL forms due to the migration of RBCs away from the wall. We take the method proposed by Fedosov et al. (2010) to calculate the thickness of CFL. We compare our simulation results with those in Zhao et al. (2012). It is found that there is good agreement between them. It also indirectly confirms that our model of interactions between RBCs is accurate.

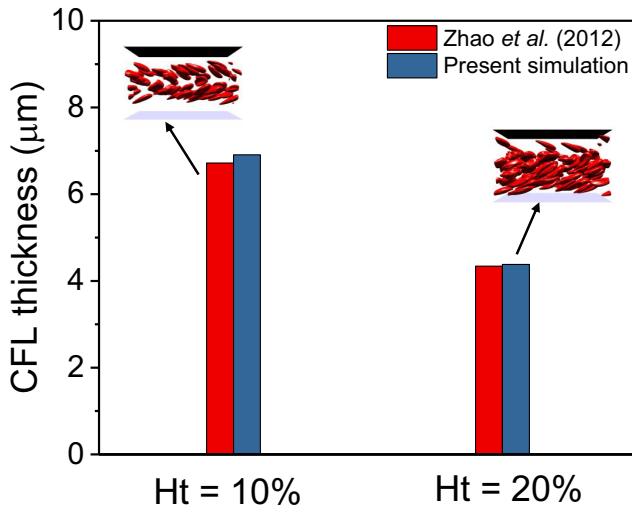


Figure 3. Comparison of the cell-free layer (CFL) thickness for hematocrit $Ht = 10\%$ and 20% between Zhao et al. (2012) and present simulations.

4. Periodic boundary condition and length effect of the channel

To investigate the boundary condition effect on the margination of MPs, we first confine the channel in the width direction (x -direction) as shown in figure 4(a). We choose a typical case $Ca = 0.037$ with no adhesion effect. And we calculate the margination probability of MPs in the channel. The result in figure 4(c) shows that the confinement in width direction can enhance the margination of MPs, though the enhancement is relative small. Then we double the length of channel from $54 \mu m$ to $108 \mu m$. We find that the margination probability result keeps almost the same as that in the short channel shown in figure 4(d). It means that the length $54 \mu m$ is large enough when considering the margination behavior of MPs in present study.

Because many in vitro experiments adopt the periodical boundary condition in width direction due to easy control of manufacturing and flow rate, we also apply the periodic boundary condition in width direction. Although it has a small influence on the margination result, there should be the same trend when considering the MP stiffness and adhesion effects. As for the channel length, current length is long enough to ensure either computation accuracy and cost.

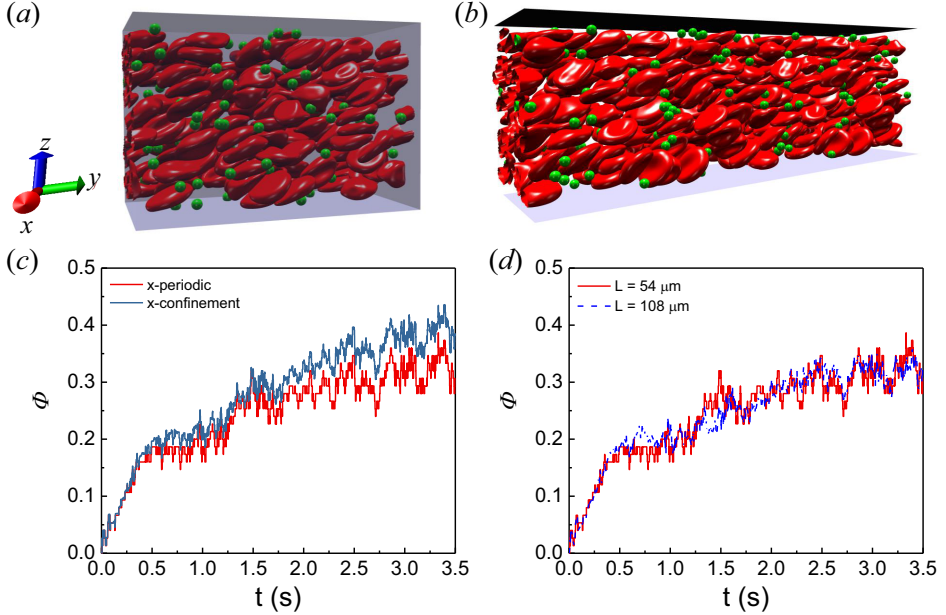


Figure 4. Effects of boundary conditions on margination behavior of MPs. (a) Applying confinement in x -direction. (b) Double length of the channel in flow direction (y -direction). (c) Comparison of margination results for case $Ca = 0.037$ with no adhesion effect between periodical and confined boundary conditions. (d) Effect of channel length in flow direction on the MP margination results.

5. Identification of adhesion types for MPs

The different adhesion types of MPs such as firm adhesion, stop-and-go motion, stable rolling and free motion are identified by calculating their velocity evolution. First, we calculate the evolution of velocity of the MP along the flow direction. We define index I_i as

$$I_i = \begin{cases} 1, & \text{if } v_c^i > 0.01V_{center}, \text{ move} \\ 0, & \text{if } v_c^i \leq 0.01V_{center}, \text{ stop} \end{cases}, \quad (5.1)$$

where v_c^i is the velocity of MP's center at time i , and V_{center} is the velocity of the flow at the center of MP. Then we can calculate the average stop time $\tau_{stop} = \Delta t \sum_{i=1}^T (1 - I_i) / T$, where T is the total simulation time. And the average velocity is:

$$\bar{v}_c = \frac{1}{T} \sum_{i=1}^T v_c^i. \quad (5.2)$$

In the simulation, we perform 1.4 s simulation in total. The motion types are defined as: $\tau_{stop} > 0.5$ s for firm adhesion; 0.1 s $< \tau_{stop} < 0.5$ s for stop-and-go motion; $\tau_{stop} < 0.1$ s and $\bar{v}_c < 0.8V_{center}$ for stable rolling and $\tau_{stop} < 0.1$ s and $\bar{v}_c > 0.8V_{center}$ for free motion.

6. Computational cost

Because the vasculature in the human body is very complex, only part of the blood vessel is adopted to study the dynamics of MPs in blood flow when considering the effect of RBCs. This can save the computational cost and simplify the modeling process, and it can ensure the accuracy to predict the motion of MPs in blood flow. Here, the Eulerian

Simulation	Number of simulations	Time step	Simulation time (s)	wall-clock time (hours)	Number of CPU cores (Intel Xeon Platinum 8160)
Margination without adhesion	5	500,000	6.5	42	576
Margination with adhesion	35	500,000	6.5	48	576
Adhesion of a single MP	35	110,000	1.4	11	576
Pair collision experiment	5	8000	0.1	0.75	576

Table 1. Computational cost of our simulations.

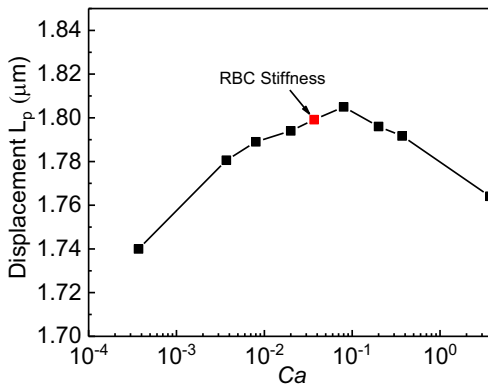


Figure 5. Displacement of a MP in pair collision with RBC. The red solid rectangle represents the MP with the same stiffness of RBC.

fluid grids in the study of margination behavior of MPs is $108 \times 216 \times 144 = 3,359,232$. Solving the Navier-Stokes equations takes about 68% of the total simulation time. About 13% computational time is consumed by the coarse-grained model for RBCs and MPs. Others are used by such as communications among CPUs, writing results and creating neighbor lists. There are total 40 simulations for the studies of margination of MPs in blood flow. It takes 48 hours to accomplish one simulation for 500,000 timesteps using 576 CPU cores (Intel Xeon Platinum 8160). The physical shear rate is 200 s^{-1} . And we perform about 6.5 s in physical time for each simulation. For the adhesion study of a single MP on substrate and pair collision numerical experiments, we summarize the simulation time and overall wall-clock time in Table. 1. All of our simulations use the same channel dimension and shear rate. Hence, we use the same number of CPU cores to solve the fluid dynamics. Margination simulation of MPs with and without adhesion performs long enough to reach the statistical equilibrium state. The adhesion of a single

MP and pair collision experiment only takes a small portion of totally computational cost, because they need shorter time to reach steady-state regime.

7. Pair collision between RBC and MP

To systematically investigate the displacement L_p of MP in pair collision with RBC, more numerical experiments for MPs with different stiffnesses are conducted. From the figure 5, we find that the displacement of MP increases with the increment of Ca , and the displacement decreases after Ca exceeds a critical value Ca_c . Ca_c is a little bit larger than the corresponding Ca of RBC. It means when the MP is slightly softer than the RBC, the displacement L_p reach its maximum value.

REFERENCES

- Fedosov, Dmitry A, Caswell, Bruce, Popel, Aleksander S & Karniadakis, George Em 2010 Blood flow and cell-free layer in microvessels. *Microcirculation* 17 (8), 615–628.
- Fedosov, Dmitry A, Pan, Wenxiao, Caswell, Bruce, Gompper, Gerhard & Karniadakis, George E 2011 Predicting human blood viscosity in silico. *Proceedings of the National Academy of Sciences* 108 (29), 11772–11777.
- Lac, E, Barthes-Biesel, D, Pelekasis, NA & Tsamopoulos, J 2004 Spherical capsules in three-dimensional unbounded stokes flows: effect of the membrane constitutive law and onset of buckling. *Journal of Fluid Mechanics* 516, 303–334.
- Liu, Yaling & Liu, Wing Kam 2006 Rheology of red blood cell aggregation by computer simulation. *Journal of Computational Physics* 220 (1), 139–154.
- Tan, Jifu, Thomas, Antony & Liu, Yaling 2012 Influence of red blood cells on nanoparticle targeted delivery in microcirculation. *Soft Matter* 8 (6), 1934–1946.
- Zhao, Hong, Shaqfeh, Eric SG & Narsimhan, Vivek 2012 Shear-induced particle migration and margination in a cellular suspension. *Physics of Fluids* 24 (1), 011902.